FEATURE ARTICLE

Dynamics of Tropospheric Aerosols

Spyros N. Pandis,[†] Anthony S. Wexler,[‡] and John H. Seinfeld*[,§]

Department of Chemical Engineering and Engineering and Public Policy, Carnegie-Mellon University, Pittsburgh, Pennsylvania 15213; Department of Mechanical Engineering, University of Delaware, Newark, Delaware 19716; and Department of Chemical Engineering, California Institute of Technology, Pasadena, California 91125

Received: February 13, 1995; In Final Form: April 6, 1995[⊗]

Anthropogenic emissions leading to atmospheric aerosols have increased dramatically over the past century. Airborne particles have been implicated in human health effects, visibility reduction in urban and regional areas, acidic deposition, and altering the earth's radiation balance. The atmosphere subjects aerosol particles to an array of transport and transformation processes that alter their size, number, and composition; the transformation processes include condensation and evaporation, homogeneous nucleation, coagulation, and chemical reactions. A major goal of our research has been to use first principles to gain a predictive understanding of the physical and chemical processes that govern the dynamics, size, and chemical composition of atmospheric aerosols. We review here the current state of our ability to model this atmospheric aerosol behavior.

1. Introduction

Particles in the atmosphere arise from natural sources, such as wind-borne dust, sea spray, and volcanoes, and from anthropogenic activities, such as combustion of fuels. While an aerosol is technically defined as a suspension of fine solid or liquid particles in a gas, common usage refers to the aerosol as the particulate component only. Emitted directly as particles (primary aerosol) or formed in the atmosphere by gas-to-particle conversion processes (secondary aerosol), atmospheric aerosols are generally considered to be the particles that range in size from a few nanometers to tens of micrometers in diameter. Once airborne, particles can change their size and composition by condensation of vapor species or by evaporation, by coagulating with other particles, by chemical reaction, or by activation in the presence of water supersaturation to become fog and cloud droplets. Particles smaller than 1 μm diameter generally have atmospheric concentrations in the range from around 10 to 1000's per cm^3; those exceeding 1 μm diameter are usually found at concentrations less than 1 cm^{-3}.

The troposphere is the lowest layer of the atmosphere, ranging from the ground to an altitude of 10−15 km depending on latitude and weather conditions. The troposphere includes more than 80% of the atmospheric mass and is the atmospheric region where most weather processes occur. Because the temperature of the troposphere decreases with altitude, it is dynamically unstable. The atmospheric layer lying on top of the troposphere and extending to an altitude of around 50 km is called the stratosphere. The temperature is approximately constant in the lower few kilometers of the stratosphere and increases from approximately 20 to 50 km.

Particles are eventually removed from the atmosphere by two mechanisms: deposition at the earth's surface, so-called dry deposition, and scavenging by droplets during precipitation, so-called wet deposition. Because wet and dry deposition lead to relatively short residence times in the troposphere and because the geographical distribution of particle sources is highly nonuniform, tropospheric aerosols vary widely in concentration and composition over the earth. Whereas atmospheric trace gases have lifetimes ranging from less than a second to a century or more, the residence times of particles in the troposphere vary only from a few days to a few weeks.

The stratospheric aerosol is an aqueous sulfuric acid solution composed of 60% to 80% sulfuric acid for temperatures from −80 to −45 °C, respectively.[1] Carbonyl sulfide (COS), which has its sources at the earth's surface but is chemically inert and water-insoluble, diffuses into the stratosphere where it dissociates by solar ultraviolet radiation to form sulfuric acid, the primary component of the natural stratospheric aerosol. Carbon disulfide (CS_2) is produced during biomass burning and from wetlands but also from anthropogenic sources (automotive tire wear, etc.). CS_2, which is converted to COS in the troposphere, may also be a source of stratospheric aerosol. Some portion of these sulfur-containing compounds result from biomass burning, fossil fuel combustion, and petroleum refining. Aircraft flying in the upper troposphere/lower stratosphere constitutes an additional anthropogenic source of stratospheric particles. Polar stratospheric clouds (PSCs), consisting of microscopic ice crystals of sulfuric and nitric acid and water, serve as sites for heterogeneous chlorine reactions that lead to the ozone hole phenomenon.[2] Data obtained from measurements of the stratospheric aerosol at Laramie, WY, indicate that the background (nonvolcanic) stratospheric sulfuric acid aerosol mass at northern midlatitudes increased by about 5% per year during the 10 year period prior to the eruption of Mt. Pinatubo.[3] Whether this increase was natural or anthropogenic could not be determined. By far the largest perturbation to the stratospheric aerosol, however, is that resulting from volcanic eruptions. Volcanoes inject ash and sulfur-containing gases into

* To whom correspondence should be addressed.
[†] Carnegie-Mellon University.
[‡] University of Delaware.
[§] California Institute of Technology.
[⊗] Abstract published in *Advance ACS Abstracts*, June 1, 1995.

0022-3654/95/2099-9646$09.00/0

the stratosphere. The relatively larger ash particles fall out of the stratosphere within a few months; the sulfur-containing gases undergo gas-to-particle conversion to produce submicron sulfate aerosols that can have stratospheric lifetimes of several years. Because of their long lifetime, stratospheric aerosols are much more spatially and chemically homogeneous than aerosols in the troposphere. With an estimated aerosol mass addition of 30 Tg to the stratosphere, the June 1991 eruption of Mt. Pinatubo led to enhanced stratospheric aerosol levels for over 2 years.[4]

A significant fraction of the tropospheric aerosol is anthropogenic in origin. Chemical components of tropospheric aerosols include sulfate, ammonium, nitrate, sodium, chloride, trace metals, carbonaceous material, crustal elements, and water. The carbonaceous fraction of the aerosols consists of both elemental and organic carbon. Elemental carbon, also called black carbon, graphitic carbon, or soot, is emitted directly into the atmosphere, predominantly from combustion processes. Particulate organic carbon is emitted directly by sources or can result from atmospheric condensation of low-volatility organic gases. Anthropogenic emissions leading to atmospheric aerosol have increased dramatically over the past century[11] and have been implicated in human health effects,[5] in visibility reduction in urban and regional areas,[6-8] in acid deposition,[9] and in perturbing the earth's radiation balance.[10-12]

Particles that can become activated to grow to fog or cloud droplets are termed cloud condensation nuclei (CCN). At a given mass of soluble nucleus there is a critical value of the ambient supersaturation, below which the particle exists in a stable state and above which it enters an unstable process of spontaneous water accretion leading to a cloud droplet. These different regimes of atmospheric aerosol growth are due to the combination of the curvature increase and the solute concentration lowering of the water vapor pressure over a droplet. The number of particles that can act as CCN is thus a function of the water supersaturation. For marine stratiform clouds, for example, supersaturations are in the range of 0.1−0.5%, which corresponds to a minimum CCN particle diameter of 0.05−0.14 μm. CCN number concentrations vary from fewer than 100 cm^{-3} in remote marine regions to a few thousand cm^{-3} in polluted urban areas. Once activated, fog and cloud droplets grow to sizes exceeding 10 μm diameter.

Atmospheric aerosols influence the earth's radiation balance in two ways: (1) through the scattering and absorption of solar radiation back to space, the so-called direct effect, and (2) by acting as CCN to influence the formation, lifetime, and radiative properties of clouds, the so-called indirect effect.[10-12] Averaged over latitude and over both day and night, the solar energy received by the earth is 343 W m^{-2}. About 30% of this energy is reflected back to space, mostly by clouds, leaving 240 W m^{-2} to be absorbed. Averaged over a year, the earth is in approximate energy balance; about 240 W m^{-2} of thermal infrared radiation is emitted back to space. The globally averaged radiative forcing resulting from increases in sulfate aerosol since about 1850 is estimated to lie in the range of −0.25 to −0.9 W m^{-2}.[13] The radiative forcing from aerosols from biomass burning, again globally averaged, has been estimated to be in the range of −0.05 to −0.6 W m^{-2}.[13] For comparison, the radiative forcing resulting from increases in greenhouse gases over the same period is estimated as +2.1 to +2.8 W m^{-2}. Estimates of the radiative forcing resulting from the indirect effect of aerosols are much more uncertain than for the direct effect; it has been estimated that the indirect radiative forcing (also negative) is roughly comparable to that of the direct effect. For reference, the stratospheric aerosol perturbation from Mt. Pinatubo caused a temporary global mean peak climate forcing of about −4.0 W m^{-2}.[13] The role of aerosols is generally recognized as one of the most uncertain elements of the effect of anthropogenic emissions on climate. Aerosols may also influence the heterogeneous chemistry of reactive greenhouse gases, such as ozone.

A major goal of our research has been to gain a predictive understanding of the interactive physical and chemical processes that govern the atmospheric aerosol system relating to natural and human-induced effects of aerosols on human health, visibility, ecosystems, and climate. For example, climate models will require reliable models of climate forcing by airborne particles. Similarly, determination of the effects of anthropogenic emissions changes on urban and regional aerosol levels and composition will require accurate predictive models of aerosol behavior. The central question that underlies this goal is the following: Can we predict the size and composition, and hence radiative and hygroscopic properties, of the atmospheric aerosol?

In this article we review the current state of our ability to model atmospheric aerosol behavior from first principles. We will focus largely on the tropospheric aerosol, although the general ideas and methods employed apply equally well to stratospheric aerosols. We begin with a concise survey of the different classes of aerosols in the troposphere. We do so because, as noted above, the tropospheric aerosol is highly variable, both spatially and temporally, and aerosols in different regions of the troposphere have widely differing characteristics. We then briefly survey the key microphysical elements that govern the size and composition distribution of atmospheric aerosols. Section 4 formulates the basic conservation equation for the aerosol size/composition distribution and addresses the terms in that equation, of which gas-to-particle conversion is seen to be a principal component. In section 5 we survey the current understanding of and outstanding issues associated with the molecular routes of gas-to-particle conversion, and section 6 briefly considers cloud/aerosol interactions.

2. Tropospheric Aerosols

The relatively short residence time of aerosols in the troposphere, usually less than a week, results in significant spatial variations in particle concentration, size, and composition. In an effort to categorize tropospheric aerosols nine rough tropospheric aerosol classes can be identified: marine, remote continental, nonurban continental, urban, desert, polar, biomass burning, and background (free troposphere).[14,15] These classifications are by no means unique (see, for example, refs 16 and 17).

Marine Aerosol. In the absence of significant transport of continental aerosols, the aerosol over the remote oceans is largely of marine origin.[18] Marine atmosphere particle concentrations are normally in the range of 100−300 cm^{-3}. The aerosol size distribution is characterized by three modes: the nuclei (particle diameter $D_p < 0.1$ μm), the accumulation ($0.1 < D_p < 0.6$ μm), and the coarse ($D_p > 0.6$ μm).[15] Typically the coarse particle mode, comprising 95% of the total mass, but only 5−10% of the particle number, results from the evaporation of sea spray produced by bursting bubbles or wind-induced wave breaking.[19,20] Typical sea-salt aerosol concentrations in the marine boundary layer[21,22] (MBL) are thought to be around 20−30 cm^{-3}.

The source of submicron non-sea-salt (nss) marine aerosol is gas-to-particle conversion of sulfuric and methanesulfonic acids resulting from the oxidation of dimethylsulfide (DMS) emitted from the ocean.[23] DMS, a metabolic byproduct of marine phytoplankton, enters the MBL at the air−ocean

interface. Its major sink is reaction with the hydroxyl (OH) radical resulting in the production of both SO_2 and methanesulfonic acid (MSA).[24,25] Uncertainty still surrounds the exact mechanism of DMS oxidation.[26,27] The SO_2 produced from the DMS−OH initiated photooxidation is homogeneously oxidized, also by the OH radical, to produce H_2SO_4 vapor that either undergoes binary heteromolecular nucleation with H_2O to form new particles or condenses on preexisting ones.[28−32] The nuclei grow by condensation of additional sulfuric acid, MSA, ammonia, and water.

The mechanisms for development of the so-called accumulation mode, in the size range $0.1 < D_p < 0.6\ \mu m$, are still unclear. Hoppel et al.[33,34] examined a number of possible mechanisms and concluded that the cycling of the aerosol through cloud formation and evaporation cycles is the most likely mechanism. The particles remaining after the cloud droplets evaporate are larger than the original CCN, reflecting the sulfate and associated material produced by reaction in the cloud drops. Alkaline sea-salt particles over the ocean have been proposed as an additional medium for sulfate production through the heterogeneous oxidation of SO_2 by O_3.[35]

Remote Continental Aerosol. Primary particles emitted by the biosphere (e.g., pollens, plant waxes) and the secondary oxidation products of biogenic gases (e.g., terpenes) are the main sources of remote continental aerosol.[36] Aerosol number concentrations in such regions average around $10^4\ cm^{-3}$, and mass concentrations average about $20\ \mu g\ m^{-3}$.[37−39] A typical remote continental aerosol number distribution has three modes centered at diameters about 0.02, 0.12, and 1.8 μm.[37−39]

Urban Aerosol. Urban aerosols are strongly anthropogenic in origin, with a definite signature from combustion sources. Number concentrations usually exceed $10^5\ cm^{-3}$, and size distributions typically have three modes: fine, accumulation, and coarse. The main constituents of urban aerosol are sulfate, nitrate, ammonium, elemental (EC), and organic carbon (OC) and crustal compounds (silicon, aluminum, calcium, and iron oxides). These aerosols are the result of primary emissions (EC, OC, geological material) and gas-to-particle transformation of the oxides of nitrogen, hydrocarbons, ammonia, and SO_2.

Desert Aerosol. Large amounts of dust are emitted to the atmosphere during high wind periods in deserts (Sahara, Gobi, Australian). Most of these particles are coarse ($D_p \geq 1\ \mu m$) and are thus deposited close to the source; some fraction of the smaller particles can be transported over large distances.[40] For example, dust from the Sahara is regularly detected on Barbados Island across the Atlantic ocean.[11] The chemical composition of desert aerosol is similar to that of its soil source and is often rich in calcium compounds and other alkaline elements. Desert aerosol has been estimated to significantly contribute elements such as Al, Si, or Fe to the sea.[41] The amount of dust emitted globally on an annual basis is difficult to estimate, especially as the estimate depends crucially on the definition of the upper particle size cutoff. One recent estimate for the emission flux of desert aerosol that is subject to long-range transport is 1500 Tg/yr.[42]

Polar Aerosol. Because of persistent vortices, air masses generally remain over polar ice for extended periods of time. Any large particles that are present have sufficient time to deposit out, leaving a monodisperse aerosol with a mean size of about 0.15 μm and a number concentration in the range of 15−150 particles cm^{-3}.[43] Suitable meteorological conditions leading to the transport of anthropogenic aerosol to high latitudes in winter and early spring produce the so-called Arctic Haze.[44] Transported pollutants are lowest in summer, leading to significantly cleaner air at northern latitudes as compared to the wintertime.[45] The polar aerosol is also influenced by intrusions of stratospheric air characterized by low aerosol number concentrations and a broad aerosol size distribution with a significant percentage of particles having diameters larger than 0.2 μm. There appears to be a surface source of NH_3 over the pack ice that is available to react with the acidic sulfate aerosols.[45] This NH_3 may originate from decay of dead marine organisms on the ice surface or from surface ocean waters.

Background Aerosol. The aerosol in the mid and upper troposphere, the so-called free troposphere, is often termed background aerosol. It is well-aged aerosol with a composition and size distribution that have been shaped through the simultaneous effect of long-range transport and removal processes. The number concentration of background aerosol is in the range of 30 cm^{-3},[46] and its size distribution is nearly monodisperse with peak diameters in the 0.2−0.5 μm range.[47] Regions with the lowest mass concentrations generally have the highest number concentrations,[48] suggesting that nucleation is a major source of particle number. Volatility measurements of the free tropospheric aerosol suggest a composition dominated by sulfates.[48,49]

Biomass Burning Aerosol. Remote biomass burning (forest and savanna fires, agricultural burning, etc.) is now recognized as a major source of both primary (ash, elemental carbon) and secondary (organic, sulfate, nitrate, and ammonium) aerosol. The chemical composition of the aerosol produced depends on the characteristics of the combustion; hot flaming fires (e.g., savanna fires) emit mainly EC aerosol, while smoldering fires emit mainly organic particles.[11] The number concentrations of aerosols produced by biomass fires are of the order of tens of thousands of particles per cm^3 close to the source and less than 1000 cm^{-3} after a few days of transport.[50] Mass median diameters in fresh fire plumes are typically in the range of 0.1−0.3 μm and evolve toward values in the range 0.2−0.4 μm during the first few hours after emission. A second mass peak is frequently seen over burning savanna fires and in burning biomass plumes at diameters of several micrometers. This peak may be related to entrainment of soil and ash particles due to the turbulence created by the flames.

Nonurban Continental Aerosol. Nonurban continental aerosol is often acidic as a result of anthropogenic sulfate or nitrate. The presence of significant amounts of strong acidic sulfates shifts the $HNO_3(g)$/aerosol nitrate equilibrium toward the gas phase; high $HNO_3(g)$ acid levels can be present with acidic sulfate aerosols. Typical aerosol number concentrations of nonurban continental aerosol[51] are in the range of $10^3\ cm^{-3}$, with mass concentrations around $30\ \mu g\ m^{-3}$. The aerosol mass distribution usually exhibits a trimodal structure similar to that of urban aerosol.

Despite significant progress in our understanding of the global aerosol system over the past two decades, our knowledge of the sourses and dynamics of atmospheric aerosols remains limited. Difficulties associated with measurement of the aerosol size/composition distribution, combined with the significant spatial and temporal variability of tropospheric aerosol, have resulted in only scattered knowledge of its global distribution. Aerosols in remote locations, and in the middle and upper troposphere, have received relatively little attention, and their size/composition distribution remains largely unexplored. Most of the existing measurements are ground-based, and consequently, there is a general lack of information on the vertical aerosol distribution. Moreover, few measurements of the chemical composition of the smallest atmospheric particles, e.g. smaller than 50 nm diameter, are available.

3. Aerosol Microphysics

The atmosphere subjects aerosol particles to an array of transport and transformation processes that alter their size, number, and composition. Transport processes include gravitational settling, advection by bulk motion of the air, and turbulent mixing. Transformation processes include condensation and evaporation, which result from diffusion of vapors between the particle and the interstitial gas, homogeneous nucleation to produce new particles from supersaturated vapors, coagulation, which combines two particles into one by collision and sticking, and chemical reactions occurring in individual particles. Advective and turbulent transport of particles is nearly identical to that of the interstitial gas because the characteristic particle relaxation time is typically much smaller than the Kolmogorov time scale of the turbulence. The particle relaxation time is the characteristic time for a particle to relax to the velocity of the surrounding fluid in the absence of external forces and is smaller than about 0.001 s for atmospheric particles.[52] The Kolmogorov time scale, the characteristic time for dissipation of the smallest eddies in the flow, is of the order of 10 s or more.[53]

Although each of these processes alters the atmospheric aerosol, their importance in a particular situation depends on the nature of the aerosol population and the atmospheric conditions. In this section we focus on aerosol transformation processes.

Single Particle Mass Transport. That a major portion of atmospheric aerosol mass is secondary in nature is indicative of the importance of gas-to-particle conversion. Gas-to-particle conversion processes include condensation of vapor on particles and formation of new particles by homogeneous nucleation. (Evaporation, the reverse of condensation, might be termed particle-to-gas conversion.) Here we examine condensation.

The driving force for condensation is the difference in partial pressure between vapors at the surface of the particles and in the ambient gas. Atmospheric trace gases have mixing ratios in the parts per billion (ppb) range, so dilute transport theory applies. As a result of these low concentrations, condensation is sufficiently slow that heating effects due to condensation are negligible and, consequently, the temperature difference between the particle and gas is insignificant. Finally, the gas-phase concentration profile around the particle establishes a steady state on the order of 10^{-3}s, so a pseudo-steady-state mass flux analysis can be employed.[54] The factors that govern the rate of condensation to a single particle depend on the size of the particle relative to the mean free path of the ambient air, λ—the mean free path of air is about 0.07 μm at 298 K while the particle diameters of interest range from 0.001 to 10 μm. When the particle is sufficiently small relative to the mean free path, free molecular theory applies and the single particle mass flux is given by

$$\left.\frac{dm}{dt}\right|_{fm} = \pi R_p^2 \alpha \bar{v} M \frac{p_\infty - p_{surf}}{RT} \quad (1)$$

where R_p is the particle radius, α is the molecular accommodation coefficient, the fraction of molecules striking the surface that are absorbed, $\bar{v} = \sqrt{8RT/\pi M}$ is the root-mean-square velocity of the condensing vapor, M is its molecular weight, p_∞ is its ambient partial pressure, p_{surf} is its partial pressure above the particle surface, R is the universal gas constant, and T is the ambient temperature. For particles sufficiently large relative to the mean free path, a continuum approximation holds, and the single particle flux is

$$\left.\frac{dm}{dt}\right|_{cont} = 4\pi R_p D M \frac{p_\infty - p_{surf}}{RT} \quad (2)$$

where D is the molecular diffusivity of the vapor.

Between the free molecular and continuum limits lies the so-called transition regime. No general analytical solution to diffusion in the transition regime is available, but a number of approximate solutions have been developed using, for example, Grad's moment solution to the Boltzmann equation or by simply matching the free molecular and continuum solutions.[55-62] The simplest transition regime transport equations depend only on the Knudsen number ($Kn \equiv \lambda/R_p$) and the accommodation coefficient, while more exact solutions also include the ratio of the molecular weights of the condensing and carrier gases (for reviews see refs 63 and 64). For very small values of the accommodation coefficient the transition regime flux correction scales as α/Kn. Thus, for very small α, the transition regime actually extends to large particle sizes (small Kn).

The solutions referred to above apply to condensation of a single compound on a spherical particle, but not all atmospheric particles are spherical and not all condensation or evaporation processes are strictly unimolecular. Under sufficiently dry conditions, certain particles may form faceted solid crystals, and often fresh emissions from combustion sources are in the form of chain agglomerates. Recent progress has been made to characterize condensation rates on particles of irregular shape.[65] Bimolecular condensation can take place when two vapors condense to form a solid crystal in fixed stoichiometry. For instance, ammonia and nitric acid condense to form ammonium nitrate in a one-to-one stoichiometry; most current condensation theories are not designed to handle this more complicated particle surface boundary condition.[61]

The accommodation coefficient α is a measure of the kinetic limitation to condensation at the particle surface, which is governed by a number of factors including the condensing species, and the composition and morphology of the particle. A large uncertainty, sometimes more than an order of magnitude, exists in our knowledge of their values. Most accommodation measurements have been carried out for gases to or from a dilute aqueous phase typical of cloud and fog droplets.[66-68] Water—water accommodation in the atmosphere has been extensively reviewed by Mozurkewich.[69] Since cloud droplets are relatively large, mass transport is governed by molecular diffusion, and the accommodation process plays a secondary role.[70] Smaller particles often exist under conditions of lower relative humidity and therefore may be a solid, a mixture of solid and aqueous phases, or highly concentrated solutions. Few measurements of accommodation exist on highly concentrated or mixed phase particles.

The characteristic time for transport to the interior of aqueous atmospheric particles is short compared to that for vapor mass transport to the surface,[54] and consequently particles are generally assumed to be internally homogeneous for the purposes of mathematical description. This may not be the case for solid particles. In ammonium nitrate condensation, formation and thickening of an ammonium nitrate crystalline layer on the particle surface take place—the solid itself does not limit transport. But for evaporation, transport to the surface from the interior of the particles may reduce mass transport substantially. Such may have been the case in experiments performed by Hightower and Richardson,[71] who formed aqueous ammonium nitrate—ammonium sulfate particles, dried them to a solid, and measured ammonium nitrate evaporation rates that were much lower than that for pure ammonium nitrate. This result could be explained either by the formation of ammonium

nitrate−ammonium sulfate double salts or by formation of an ammonium sulfate coating surrounding the ammonium nitrate core.

Atmospheric aerosols may have surface-active organic coatings in both the urban[72] and marine environments.[73−77] Such coatings substantially reduce the accommodation coefficient of highly soluble inorganics on water.[78,79]

Single Particle Thermodynamics. Mass transport is influenced through the phase state and surface partial pressure of the condensing species, p_{surf}. In general, particle-surface partial pressure, and therefore equilibrium gas-particle partitioning, is dependent on temperature, relative humidity, and particle composition.[80,81]

The aqueous phase of atmospheric aerosols contains primarily strong electrolytes such as sodium chloride, nitric and sulfuric acids, and ammonium. At relative humidities much below saturation, the vast majority of water in the atmosphere is in the vapor phase, and therefore the liquid water associated with aerosol particles does not affect the ambient relative humidity. For relative humidities below saturation, water can be assumed to be in equilibrium between the vapor and aqueous phases because the characteristic time for water equilibration is relatively short. At equilibrium the ambient relative humidity determines the water activity in the particles. Other volatile species may or may not be in equilibrium, a point that will be discussed subsequently.

With a single aqueous phase containing dissolved electrolytes, when compounds condense or evaporate, water must also condense or evaporate to maintain the particle water activity equal to the ambient relative humidity. Thus, the water content of particles changes in response to condensation or evaporation of electrolytes or in response to changes in ambient relative humidity itself (Figure 1). At a fixed electrolyte content, as the ambient relative humidity is lowered, water evaporates from the particle to maintain equilibrium. If the relative humidity is lowered sufficiently, a solid crystalline phase may form when one or more of the electrolytes reaches saturation. For instance, if the particle contains sodium chloride, this solid phase will occur theoretically at 75% relatively humidity. This defines the efflorescence point, which, according to equilibrium thermodynamics, is equivalent to the deliquescence point—the efflorescence point defines the relative humidity where the aqueous to crystalline phase transition occurs, whereas the deliquescence point defines that of the crystalline to aqueous transition. In general, the deliquescence point is a function of temperature, and this dependence can be derived from the Clausius−Clapyron equation.[82,83] The efflorescence and deliquescence points generally do not coincide because nucleation of the new crystalline phase is not thermodynamically preferred until the solution is substantially supersaturated. As a result of the supersaturations required to obtain efflorescence, this point is often referred to as the crystallization relative humidity.

For single salt solutions, there is a single deliquescence point separating the higher relative humidities where the particle is aqueous from the lower relative humidities where the particle is crystalline. Aqueous particles containing, for instance, sulfuric acid do not display a deliquescence point because no solid phase of sulfuric acid exists for typical tropospheric temperature ranges.

If the particle contains multiple salts, or combinations of salts and acids, there is a range of relative humidities where aqueous and solid phases can coexist in equilibrium (see Figure 1). Consider, for example, two salts in solution. As the relative humidity is lowered, eventually one of the salts becomes saturated and forms its crystalline phase. As the relative

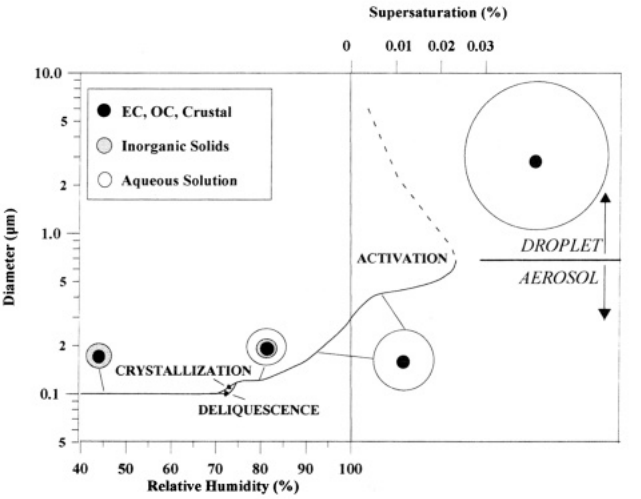

Figure 1. Schematic of the growth of a typical aerosol particle with increasing relative humidity predicted by aerosol thermodynamics. The dry particle initially consists of 16% Na_2SO_4, 38% $(NH_4)_2SO_4$, 35% crustal elements, 3% elemental, and 8% organic carbon. The particle remains solid until the relative humidity exceeds its deliquescence point (68%). The particle consists at this relative humidity regime (67−72%) of a solid core of Na_2SO_4, $(NH_4)_2SO_4$, crustal elements, EC, and OC surrounded by an aqueous solution of SO_4^{2-}, HSO_4^-, NH_4^+, Na^+, and NO_3^- from the dissolution of gas-phase HNO_3. As the relative humidity increases above 72%, the solid Na_2SO_4 and $(NH_4)_2SO_4$ dissolve completely, and more gas-phase NH_3 and HNO_3 are transferred to the aerosol phase. When the relative humidity reaches 100%, the particle diameter has increased by a factor of 3 and the particle growth becomes exponential. All the available HNO_3 and NH_3 have been transferred to the aerosol phase. The aerosol continues to be in equilibrium with the gas phase until the relative humidity reaches a critical value (100.023% for this particle). There are no equilibrium states above this threshold relative humidity (dashed line). All states are unstable, and the particle diameter is determined by the dynamics of water condensation. The particle diameter increases by a factor of 100 or more, the aerosol becomes a droplet, and water is removed to a sufficient extent from the vapor phase that the relative humidity drops.

humidity continues to decrease, more of this salt precipitates, and the solution becomes simultaneously more concentrated in the nonprecipitating salt. Eventually the nonprecipitating salt reaches its saturation, and further decreases in relative humidity cause the particle to completely effloresce.[82] If the particle contains a salt and an acid, the first deliquescence will occur, but the aqueous phase will continue to persist due to the absence of a deliquescence point for the acid. Using the Gibbs−Duhem relation, it has been shown that the deliquescence points of nonreacting mixtures are always lower than that of single solutes.[82]

Calculation of solute activities in highly concentrated aqueous solutions close to the deliquescence point is difficult. For example, at 298 K, the concentration of ammonium nitrate at saturation is over 25 *m*, which corresponds to 60% relative humidity. The use of the electrodynamic balance has allowed measurement of water activities in highly concentrated, even supersaturated, single-solute solutions,[84−86] and a few measurements of mixtures at these high concentrations are available.[85,87−89] These measurements have been used with the ZSR mixing rule and one or more solute activity models[90−94] to estimte solute activity and thereby calculate its phase partitioning and surface partial pressure. Nevertheless, extrapolations to complex multicomponent solutions at these high concentrations are highly uncertain and in need of substantial further work.

Organic coatings have been reported to reduce the deliquescence relative humidity of NaCl particles, to decrease the water absorbed by the particle, and to render hydrophobic carbonaceous particles partially hydrophilic.[95] These findings stress

the need for more experimental information on the effects of coating aerosol particles with organic material.[96]

In this section we have discussed single particle mass transport and thermodynamics. The largest uncertainty in predicting mass transport to submicron particles is the accommodation coefficient. Predicting the phase state and surface partial pressure of semivolatile compounds also presents considerable challenges because of the substantial nonideality of the solution. In the next section we will examine mass transport to a population of particles.

Particle Population Mass Transport. To determine how a particle population changes as a result of mass transport, first we write the single particle mass transport of species i as

$$\frac{dm_i}{dt} = 4\pi R_p D_i M_i \frac{p_{i,\infty} - p_{i,surf}}{RT} F(Kn,z) \qquad (3)$$

where $F(Kn,z)$ is the noncontinuum correction, and $z = M_i/M_{air}$ is the molecular weight ratio of condensing to carrier gases.

The ambient partial pressure, $p_{i,\infty}$, changes as a result of simultaneous condensation, evaporation, or both onto the population of particles. Integrating the single particle mass transport rate (see eqs 1 and 2) over the particle size distribution gives the change in ambient partial pressure

$$dp_{i,\infty}/dt = 4\pi D_i \int n(R_p) R_p (p_{i,\infty} - p_{i,surf}) F \, dR_p \qquad (4)$$

where $n(R_p)$ is the number distribution of particles. Note that n, $p_{i,surf}$, and F are functions of R_p.

It is frequently assumed that thermodynamic gas–aerosol equilibrium holds for volatile species when modeling phase partitioning. To assess the validity of this assumption, one can define and evaluate the characteristic times over which the vapor and particles equilibrate. Two equilibration time constants are relevant—one corresponding to changes in the vapor concentrations and the other to changes in the particle surface partial pressures.

Using eq 4, we can define the time constant for achieving particle–vapor equilibrium resulting from changes in the vapor-phase concentrations as

$$\tau_\infty^{-1} \equiv \frac{1}{p_{i,\infty}} \frac{dp_{i,\infty}}{dt} = 4\pi D_i \int n(R_p) R_p \frac{p_{i,\infty} - p_{i,surf}}{p_{i,\infty}} F \, dR_p \qquad (5)$$

This time constant has two components. The term $(p_{i,\infty} - p_{i,surf})/p_{i,\infty}$ is a dimensionless measure of the driving force that returns the system to equilibrium. For nonvolatile species this quantity has a maximum value of unity, and for species in particle–vapor equilibrium it is identically zero. For accomodation-limited situations, the remaining terms are proportional to the accommodation coefficient and the aerosol surface area.

Figure 2 shows the magnitude of τ_∞ as a function of particle number concentration and size assuming an accommodation coefficient α_i of 0.1, $(p_{i,\infty} - p_{i,surf})/p_{i,\infty} = 1$, and a monodisperse aerosol. Smaller particles at higher concentrations present more opportunity for condensation, so τ_∞ is small, whereas larger particles at low concentration yield a long time constant. The aerosol can be considered to be in particle–vapor equilibrium if the time constant over which vapor-phase concentrations change in the atmosphere is significantly longer than τ_∞.

The time constant for equilibration as a result of surface partial pressure changes is more difficult to evaluate because it is a function of the particle composition. Thus, a different time

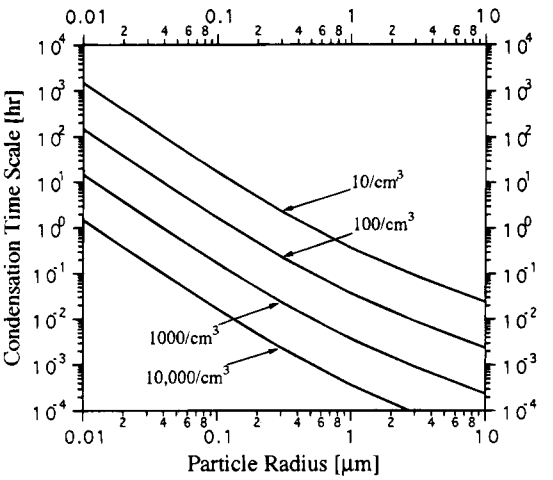

Figure 2. Characteristic time for achieving particle–vapor equilibrium as a function of particle radius and aerosol number concentration.

constant is associated with each unique particle size and composition. This is further complicated because it is often the case that this time constant is infinite. Consider, for example, the case of a particle that contains solid ammonium nitrate. Condensation or evaporation of ammonium nitrate on the particle does not change its surface partial pressure, which yields an infinite value for an appropriately defined time constant. Infinite values of this time constant are also found for certain aqueous-phase particles.[61,97]

In summary, mass transport between the vapor and particle phases changes the vapor phase concentrations and may also change the particle surface partial pressures. The time constant for equilibration of the vapor phase provides an upper limit for the time to reach equilibrium because the particle time constants may be shorter. Particle–vapor equilibrium can be assessed by comparing the value of the equilibration time constants to the characteristic times over which changes in the vapor and surface partial pressures occur. This comparison is also very useful in assessing the probability of nucleation occurring in the atmosphere.

Nucleation. Much nucleation research relevant to the atmosphere has been focussed, via measurement and theory, on the binary nucleation of sulfuric acid and water.[98] Although a classical theory of binary nucleation of sulfuric acid and water exists,[99] substantial uncertainty still remains as to how accurately this classical theory represents the actual nucleation process. Measured nucleation rates can differ from theoretically predicted values by several orders of magnitude. From the point of view of atmospheric applications, significant nucleation rates can be defined as those exceeding 1 nucleus cm^{-3} s^{-1}. Using this nucleation rate, Jaecker-Voirel and Mirabel[99] evaluated, from classical binary nucleation theory, the critical sulfuric acid concentration at which this rate of nucleation occurs as a function of temperature and relative humidity. A numerical fit of the Jaecker-Voirel and Mirabel data for lower tropospheric conditions yields

$$C_{crit} = 0.16 \exp(0.1T - 3.5rh - 27.7) \qquad (6)$$

where C_{crit} is expressed in $\mu g \, m^{-3}$, T is temperature in kelvin, and rh is the relative humidity on the 0–1 scale.[100] The critical concentration, C_{crit}, will be low, favoring nucleation, when the ambient relative humidity is high and when the temperature is low. When the ambient sulfuric acid concentration exceeds this value, significant nucleation is expected because the nucleation rate is an extremely steep function of sulfuric acid concentration.

TABLE 1: Aerosol Processing Time Scales

process	time scale formula[a]	urban	remote marine	free troposphere	nonurban continental
transport	L/V or H^2/K_z	2−5 days	1−2 weeks	3 days−2 weeks	1−2 weeks
condensation	$[4\pi D_i \int n(R_p) R_p F\, dR_p]^{-1}$ (eq 5)	0.01−1 hour	1−10 hours	2−20 hours	0.5−20 hours
coagulation (3 nm)	$[4\pi D_s \int n_l(R_{pl}) R_{pl} \beta\, dR_{pl}]^{-1}$ (eq 7)	0.1−1 hour	5−15 hours	~1 day	1−3 hours
coagulation (30 nm)	same	0.1−2 days	10−30 days	~50 days	1−5 days
sulfate production (aerosol)	$M_{S(VI)}/[W_L(k_{H_2O} p_{H_2O_2} + k_{O_3} p_{O_3}) p_{SO_2}]$	1 week	0.1−1 day	3 weeks	1−3 weeks
sulfate production (fog)	same	0.1−1 hour	0.01−3 hours	N/A	1 hour
sulfate production (cloud)	same	0.5−5 hours	0.01−3 hours	N/A	1 hour
sulfate production (vapor)	$M_{S(VI)}/[k p_{OH} p_{SO_2}]$	0.1−5 days	1−3 weeks	1−3 weeks	1−3 weeks
deposition (~0.3 μm)	H/v_d	~1 month	~1 month	N/A	~1 month
deposition (<0.03 or >3 μm)	H/v_d	0.5−10 days	0.5−10 days	N/A	0.5−10 days

[a] L = characteristic horizontal extent of region; V = characteristic horizontal velocity; H = mixing layer depth; K_z = characteristic vertical eddy diffusivity; v_d = deposition velocity; $M_{S(VI)}$ = typical aerosol sulfate concentration; W_L = liquid water content; $p_{H_2O_2}$, p_{OH}, p_{SO_2}, and p_{O_3} = ambient partial pressures; k = SO_2 + OH gas-phase reaction rate constant; $k_{H_2O_2}$ = S(IV) + H_2O_2 pH-dependent rate constant (includes solubility of gases); k_{O_3} = S(IV) + O_3 pH-dependent rate constant (includes solubility of gases).

Sulfuric acid vapor is generated in the atmosphere by photochemical oxidation of SO_2, resulting in a concentration most frequently governed by competition between this production process and removal via condensation on preexisting particles or drops or, perhaps, deposition to the ground. Nucleation of sulfuric acid and water is preferred (a) in the daytime because photochemical processes lead to sulfuric acid vapor, (b) when the preexisting aerosol loading is low such that condensation is minimized, and (c) when the relative humidity is high and temperature is low as this combination of conditions reduces the critical concentration where nucleation is expected to occur. Calculation of the sulfuric acid vapor concentration and comparison to the critical concentration have pointed to a number of situations where nucleation is favored, including those occurring in coastal regions of Los Angeles and rural locations,[100] in post-fog conditions,[101] in the marine troposphere during rapid increases in relative humidity,[102] and in combustion-related plumes.[103]

Coagulation. Coagulation is the process whereby two particles collide and stick to form a single particle. Atmospheric processes that may lead to particle collisions include Brownian motion, turbulent shear, and differential settling. The latter two can be shown to be much less effective in this regard than Brownian motion.[100]

To evaluate the influence of Brownian coagulation on atmospheric aerosols, let us consider both coagulation of similar sized particles (self-coagulation) and coagulation of particles of disparate size. Atmospheric particles span the 10 nm to 10 μm diameter size range, so the corresponding mass range spans 9 orders of magnitude. Small particles coagulating with larger ones do not significantly increase the mass of the larger particles as much as they reduce the number of small particles. In this limit of coagulation of a very large particle with a very small particle, the coagulation rate is governed by the diameter of the large particle and the diffusivity of the small particle and can be written as $4\pi R_{pl} D_s n_s n_l \beta$, where D_s is the diffusivity of the small particle, n_s and n_l are the numbers of small and large particles, respectively, and β is a factor that accounts for noncontinuum effects and imperfect sticking efficiency. In this light, coagulation of small particles on larger ones can be likened to molecular condensation. The inverse of the time constant for depletion of small particles by coagulation on a distribution of large particles can then be defined as

$$\tau_c^{-1} \equiv \frac{1}{n_s}\frac{dn_s}{dt} = 4\pi D_s \int n_l(R_{pl}) R_{pl} \beta\, dR_{pl} \quad (7)$$

which, when evaluated, yields time constants much longer than those for molecular condensation primarily because the diffusivity of the small particles is inevitably much smaller than that of molecules.[100]

Interestingly, the time for self-coagulation, also defined by eq 7, is the age of the aerosol itself: $\tau_{sc} = \tau_{sc}^0 + t$, where τ_{sc}^0 is the initial value of the self-coagulation time constant and t is time. Thus, self-coagulation eventually turns itself off. The characteristic time of self-coagulation in the atmosphere is longer than that for dissimilar sized particles. In atmospheric aerosol dynamics coagulation does not play a significant role unless number concentrations are extremely high and/or residence times are extremely long.

Aerosol Process Time Scales. Table 1 summarizes the range of time scales for aerosol processes in different atmospheric regions. By identifying the aerosol processes that transform particles in the atmosphere, we can propose comprehensive mathematical models that may predict their size and composition. Such models are discussed in the next section.

4. Modeling Atmospheric Aerosol Dynamics

Mathematical models have been extensively employed to understand gas-phase chemical dynamics on spatial scales ranging from urban to global. Mathematical models of aerosol behavior are not nearly as well developed.

Ambient air contains on the order of 1 to 10^5 particles per cm^3, depending on the location and proximity to emission sources. Within a population of particles, the diameter ranges from a few nanometers to tens of micrometers for nonactivated particles, whereas droplets range up to 100 μm diameter or so. Over the complete size range, the particle composition may be highly variable.

The dynamic behavior of a spatially homogeneous aerosol is described by the so-called aerosol general dynamic equation,[104]

$$\frac{\partial n(m,t)}{\partial t} = -\frac{\partial}{\partial m}[I(m,t)\, n(m,t)] + \frac{1}{2}\int_0^m K(m,m-m')\, n(m',t)\, n(m-m',t)\, dm' - n(m,t)\int_0^\infty K(m,m')\, n(m',t)\, dm' + E(m,t) + N(m,t) \quad (8)$$

where m is the particle mass, $n(m,t)$ is the size distribution function at time t, such that $n(m,t)\, dm$ is the number concentration of particles having masses in the range $[m, m + dm]$, $K(m,m')$ is the coagulation coefficient for particles with mass m and m', $I(m,t)$ is the rate of change of particle mass resulting from condensation and evaporation, $E(m,t)$ is the rate of emission of particles, and $N(m,t)$ is the rate of production by homogeneous nucleation.

The degree of composition homogeneity of particles of a given size is termed the mixing characteristic of the aerosol. An externally mixed aerosol refers to the limit in which each particle is composed of only one compound. An internally mixed aerosol is the opposite extreme where all particles of a given size have the same composition. The atmospheric aerosol composition is usually somewhere between the two extreme limits. At a given size aerosol particles consist of a mixture of compounds, but their composition differs from particle to particle depending on their emission source and atmospheric history. Our knowledge of the composition distribution of atmospheric particles is limited by available analytical methods.[105] On-line single particle analytical instruments are in their infancy.[106-110] Most size-resolved aerosol measurements collect all particles of a given size and analysis is carried out on the mixture. Thus, particle-to-particle composition variations are not typically available, so for the purposes of mathematical analysis one normally assumes that the aerosol is internally mixed. Although not justifiable under all circumstances, this assumption enables one to obtain much useful insight into how the atmospheric aerosol behaves.

Condensation, evaporation, and nucleation are generally the significant transformation processes influencing aerosol mass in the urban and regional atmosphere (Table 1). Pilinis[111] derived a general multicomponent mathematical description of the size and composition of internally mixed aerosol particles undergoing condensation and evaporation. Previous formulations have either assumed particle−vapor equilibrium[104] or a single component aerosol.[112] Atmospheric particle measurements are typically reported in log-diameter coordinates because particle size varies over such a large range. Using such coordinates in a mathematical model facilitates both numerical solution and comparison with data. The spatially-dependent, logarithmically transformed equation for conservation of mass for an internally mixed aerosol is[100]

$$\frac{\partial p_i(\mu,\mathbf{x},t)}{\partial t} \quad \text{(local rate of change)}$$

$$+ \mathbf{V}(\mathbf{x},t)\cdot\nabla p_i(\mu,\mathbf{x},t) \quad \text{(spatial advection)}$$

$$= H_i(\mu,\mathbf{x},t)\, p(\mu,\mathbf{x},t) - \frac{1}{3}\frac{\partial H p_i(\mu,\mathbf{x},t)}{\partial \mu} \quad \text{(condensation/evaporation)}$$

$$+ \nabla\cdot(\mathbf{K}(\mathbf{x},t)\, \nabla p_i(\mu,\mathbf{x},t)) \quad \text{(spatial diffusion)}$$

$$+ E_i(\mu,\mathbf{x},t) \quad \text{(emissions)}$$

$$+ N_i(\mu,\mathbf{x},t) \quad \text{(nucleation)} \qquad (9)$$

where $p = \sum_i p_i$ and $p_i\, d\mu$ is the mass of compound i in the size range μ to $\mu + d\mu$, $\mu = \ln(R_p/R_{p0})$ is the log-radius size coordinate, and R_{p0} is a reference particle radius typically taken to be 1 μm, $\mathbf{x}$ are the three Cartesian spatial coordinates, and $\mathbf{V}$ is the corresponding wind velocity vector, $H_i = (1/m)(dm_i/dt)$ is the normalized condensation rate of compound i and $H = \sum_i H_i$, $\mathbf{K}$ is the turbulence diffusivity tensor, and E_i and N_i are the emission and nucleation rates of compound i, respectively.

Equation 9 governs the temporal, spatial, and size-resolved composition of an atmospheric aerosol, for which coagulation has been neglected and, as such, has five independent variables, and one dependent variable for each aerosol-phase compound. A more complete formulation that makes no assumption about the internal/external mixing characteristics of the aerosol would require only one dependent variable, usually the particle number distribution, that is, however, a function of one temporal and three spatial independent variables, plus one independent variable for each compound.[113] There are typically of order 10 major constituent classes of atmospheric particles so such a model would require 14 independent variables.

As in most atmospheric chemical models, each term in eq 9 is solved separately using operator splitting.[114] The change in the size distribution resulting from condensation and evaporation is represented by two terms; the first increases the mass distribution as compounds condense while the second shifts the distribution to larger μ during condensation because the individual particle diameters have increased. This second term has the same form as hydrodynamic advection so numerical methods employed to solve advective transport can be exploited to solve condensation and evaporation.[100,115]

Each independent variable in eq 9 requires a set of initial or boundary conditions. The procedures used for the spatial and temporal variables are identical to those used in gas-phase atmospheric modeling. Either actual ambient measurements are employed as initial conditions or a period of simulation is used to wash out the effect of initial conditions. Horizontal boundary conditions typically use background concentration values, so it is desirable to define the modeling region such that reverse flows are contained within the boundary. At the top of the domain, boundary conditions are determined by the conditions of physical transport above the atmospheric boundary layer. At the surface, particulate and gaseous species are removed by dry deposition, and emissions there and aloft introduce fresh material. Boundary conditions on the particle size coordinate do not permit particles to grow or shrink out of the simulated size range.

Deposition of particles (and gases) to the surface takes two forms. Wet deposition is removal due to hydrometeors absorbing particles and carrying them to the surface, whereas dry deposition removes them directly by settling or diffusion. The dry deposition flux of particles to the surface, F_d, is assumed to be proportional to the concentration at a reference height, C, i.e., $F_d = v_d C$, where v_d is the so-called deposition velocity. Three processes serve to deposit particle on the surface: settling, turbulent transport, and Brownian diffusion. Since the Reynolds number is high in virtually any atmospheric flow, the air is turbulent, but a laminar sublayer exists immediately adjacent to the surface. Turbulence brings particles to the laminar sublayer, while Brownian diffusion and settling are responsible for transport through the sublayer. Small particles have a relatively large Brownian diffusion coefficient so are transported efficiently through the sublayer while larger particles move through the sublayer primarily via inertia or settling. Those in between, in the size range of 0.1 to 1 μm diameter, have a deposition velocity an order of magnitude lower than those at 0.01 or 10 μm because neither mechanism is effective.

Wet deposition involves the scavenging of particles by precipitation, and the subsequent deposition of the precipitation on the ground. Scavenging is necessary, but not sufficient, for wet deposition to occur since there are precipitation events where the drops evaporate before reaching the ground. As opposed to dry deposition, wet deposition does not impose a boundary condition on eq 9, but rather removes particles from the bulk of the air mass. Rain drops are typically in the 100 μm to 1 mm size range and thus have settling velocities and diameters much larger than those of the aerosols being scavenged. There are two scavenging mechanisms. Nucleation scavenging occurs when an aerosol particle acts as a condensation site for water so that a drop results—the aerosol particle is termed a CCN.

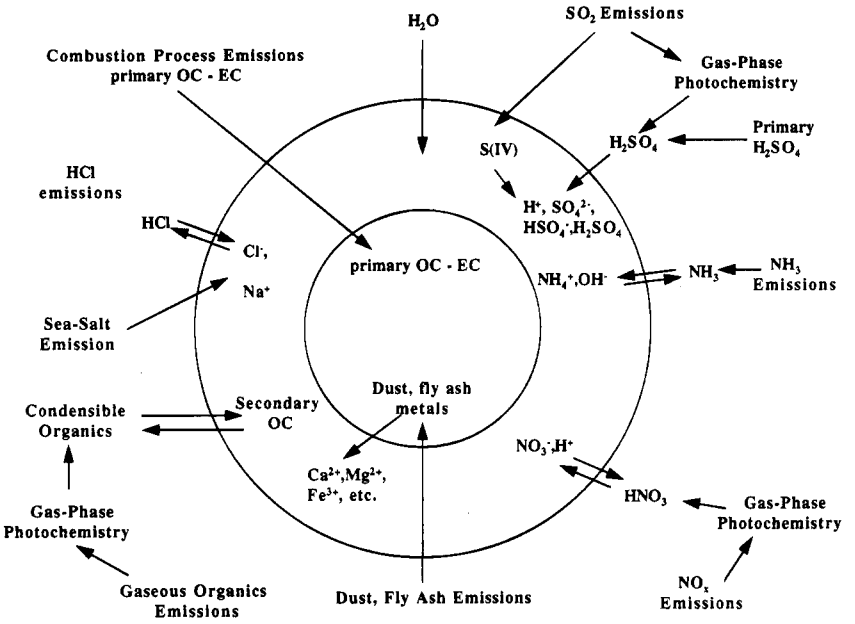

Figure 3. Sources of typical aerosol species.

Particles that are not activated to form droplets may be removed by impaction scavenging. The rate of particle collection by falling drops is proportional to the number of drops, their settling velocity, their cross-sectional area, and a collection efficiency. The collection efficiency accounts for the mechanics of particle motion in the vicinity of a falling drop and possibly inefficient accommodation. As with dry deposition, there is a minimum in the total collection efficiency in the 0.1−1 μm size range—small particles diffuse to the drop surface, larger ones collide with it, while in between neither process is very efficient.[54,116]

5. Molecular Routes to Aerosol Species

The major gaseous atmospheric precursors to aerosol species are sulfuric acid (H_2SO_4), nitric acid (HNO_3), hydrochloric acid (HCl), ammonia (NH_3), and a series of organic compounds generally containing more than 5 carbon atoms per molecule (Figure 3).

Condensable Inorganic Vapors. NH_3, HNO_3, HCl, H_2SO_4, and H_2O are the major inorganic vapors involved in the formation and growth of atmospheric aerosol. Chloride is emitted as NaCl, in primary sea-salt aerosol particles, which can react with sulfuric and nitric acids to produce gaseous HCl,

$$HNO_3(g) + NaCl(s) \rightleftharpoons NaNO_3(s) + HCl(g)$$

$$H_2SO_4(g) + 2NaCl(s) \rightleftharpoons Na_2SO_4(s) + 2HCl(g)$$

These reactions result in a chloride deficit compared to sodium in the aerosol phase, a frequent observation in both polluted and remote environments.[117]

Gas-phase ammonia can react with several acid vapors to form ammonium salts in the aerosol phase, NH_4NO_3, $(NH_4)_2SO_4$, NH_4HSO_4, $(NH_4)_3H(SO_4)_2$, and NH_4Cl. The potential main reactive inorganic components of the solid aerosol phase are therefore NaCl, $NaNO_3$, Na_2SO_4, $NaHSO_4$, NH_4Cl, NH_4NO_3, $(NH_4)_2SO_4$, NH_4HSO_4, and $(NH_4)_3H(SO_4)_2$.[104] When the relative humidity is high and the particle forms an aqueous solution, the above salts dissociate into the corresponding ions, and the aerosol components are H_2O, NH_4^+, SO_4^{2-}, NO_3^-, H^+, Na^+, Cl^-, HSO_4^-, and H_2SO_4.

Sulfuric Acid (H_2SO_4). As noted earlier, sulfuric acid is produced in the atmosphere from the oxidation of sulfur dioxide (SO_2). Once emitted, gaseous SO_2 is oxidized in the ambient troposphere to sulfuric acid by reactions occurring in the gas, aqueous, and aerosol phases. Several pathways exist for the gas-phase oxidation of SO_2 to H_2SO_4, but all available evidence suggests that the only gas-phase process that is sufficiently fast and efficient is the reaction of SO_2 with the OH radical,

$$SO_2 + OH^\bullet \xrightarrow{M} HOSO_2^\bullet$$

The effective second-order rate constant is 1.5×10^{-12} cm^3 molecule^{-1} s^{-1} at 300 K.[118] The $HOSO_2$ adduct reacts rapidly with O_2 and is thought to produce sulfur trioxide (SO_3)[119]

$$HOSO_2^\bullet + O_2 \rightarrow HO_2^\bullet + SO_3$$

with the SO_3 finally reacting rapidly with water vapor to form sulfuric acid vapor[120]

$$SO_3 + H_2O \rightarrow H_2SO_4$$

The homogeneous conversion rate of SO_2 depends on the OH concentration. Hydroxyl radicals are produced by photochemical processes—their concentration is extremely low at night and peaks around solar noon. A typical summer diurnal average SO_2 conversion rate is about 0.5% per hour in a rural atmosphere and 5% per hour in a polluted atmosphere. During winter these conversion rates are estimated to be a factor of 10 lower as a result of the lower OH concentrations.

Lovelock and co-workers[121] found dimethyl sulfide (DMS) in the ocean and proposed that it constitutes the major natural flux of sulfur from the ocean to the atmosphere; current estimates put DMS at 80−90% of the total reduced sulfur flux from the ocean, amounting to 15−30 Tg year^{-1}, about one-third of the estimated flux of sulfur from all natural sources. Charlson et al.[23] examined the sensitivity of the earth's climate to a change in the flux of DMS from the oceans. Because, as noted earlier, the dominant atmospheric fate of DMS is oxidation to sulfate, an increase in the flux of DMS can be expected to lead to a proportional increase in the mass of atmospheric non-sea-salt (nss) sulfate. And because the nss sulfate is the main

constituent of marine CCN (typical sea-salt particle number concentrations are of order 10 cm^{-3}, whereas marine stratiform cloud droplet number corrections are typically 100 cm^{-3} or more), it is conceivable that an increase in the mass of nss sulfate would cause a more or less proportional increase in the number of CCN, and thus in the number of cloud droplets, and cloud albedo.[23] If, at constant liquid water content, the number of cloud droplets over the ocean is increased by 30%, the increase in shortwave albedo at the top of the atmosphere averaged over the earth's surface is 0.005. An increase of planetary albedo by 0.005 is, in the absence of climate feedbacks, equivalent to a decrease of the solar constant by 0.7%, and climate models predict such a decrease would lead to a global mean surface air temperature decrease of 1.3 °C, about one-third the increase predicted for a CO_2 doubling.

Several components of the so-called CLAW hypothesis, after the authors of the paper, have been verified by laboratory and field measurements.[18,48,122,123] The large number of the DMS–CCN system components and their spatial and temporal variability have made it difficult to quantify through measurements alone the relationship between DMS fluxes and cloud albedo. Despite laboratory studies[24,25] the transformation of DMS to H_2SO_4 in the marine atmosphere is not well understood. It is currently believed that SO_2 is the major product, with yields increasing with temperature from 0.7 to 0.95, and methanesulfonic acid (MSA) is the secondary product.[30] However, Berresheim et al.[26] recently suggested that the dominant oxidation product of DMS may be dimethyl sulfone ($DMSO_2$), and Bandy et al.[27] proposed that the major pathway for oxidation of DMS to H_2SO_4 occurs via SO_3, not SO_2; Lin and Chameides[124] showed that such a mechanism is compatible with MSA/sulfate measured in remote marine air.

An effective approach is to probe the theoretical basis for the DMS/CCN link by developing models incorporating all of the appropriate chemical and physical processes. Kreidenweis and Seinfeld[125] and Kreidenweis et al.[28,29] proposed a framework for such a model using a three-variable aerosol parametrization and tested it against smog chamber experiments on DMS photoxidation. Pandis et al.[30] extended this framework and showed theoretically that for DMS fluxes higher than a certain threshold value, a linear relationship exists between the DMS flux and the CCN concentration. Using the results of Pandis et al.[30] coupled with the calculations of Lawrence,[126] one estimates that the DMS feedback is sufficient to offset around 50% of the greenhouse gas climate forcing. The ability to accurately quantify this effect is constrained by a number of uncertainties.[31] For example, the inability to quantify the H_2SO_4/H_2O nucleation rate in the marine atmosphere and the lack of knowledge of the H_2SO_4 accommodation coefficient on aerosol particles limit our ability to model the DMS/CCN link. Finally, the inability to model the lifetimes of marine stratus clouds makes it difficult to close the DMS–cloud albedo loop.

Nitric Acid (HNO_3). Nitric acid is formed in the atmosphere in the reaction of NO_2 with OH,[127] reaction of the NO_3 radical with organics,[128] and N_2O_5 hydrolysis. The OH–NO_2 reaction,

$$NO_2 + OH^{\bullet} \xrightarrow{M} HNO_3$$

is the most important HNO_3 source in the atmosphere; the recommended effective bimolecular reaction constant at 300 K is 2.4×10^{-11} cm^3 $molecule^{-1}$ s^{-1}.[118] A typical conversion rate of NO_x to nitric acid by this rate is about 8% per hour in the rural atmosphere or 4% per hour averaged over the whole day. Thus, in the summer most of the NO_x is converted to HNO_3 in 1 day.

Ammonia (NH_3). NH_3 plays a significant role in atmospheric chemistry because it is the only ubiquitous highly soluble basic gas present in the atmosphere. It is produced mainly by biological processes and hence exists in both clean and polluted environments. It reacts slowly with OH

$$NH_3 + OH^{\bullet} \rightarrow NH_2^{\bullet} + H_2O$$

(rate constant 1.6×10^{-13} cm^{-3} $molecule^{-1}$ s^{-1} at 298 K[118]) with an atmospheric lifetime from this reaction of the order of 70 days. Photochemical conversion is therefore a negligible sink for NH_3. Ammonia is transferred to the particulate phase reacting with sulfuric, nitric, and hydrochloric acids. The lifetime of ammonia in the troposphere is of the order of 3–5 days.

Condensable Organic Vapors. During the atmospheric oxidation of organic gases by OH, O_3, and NO_3, low vapor pressure products are formed that can then condense to the aerosol phase as secondary organic aerosol material.[129–132] Organic aerosols formed by gas-phase photooxidation of hydrocarbons have been identified in both urban and rural atmospheres. Aliphatic organic nitrates,[133] dicarboxylic acids, including adipic and glutaric acids,[134] carboxylic acids derived from aromatic hydrocarbons, such as benzoic and phenylacetic acids, and others have been identified. Most low molecular weight organics do not generate condensable compounds under photooxidation. Some condensable material can be formed from the more reactive branched alkenes having more than six carbon atoms, e.g., isooctane. Alkenes with fewer than six carbon atoms do not form aerosol; those with six or more carbon atoms form aerosol when they yield, after rupture of the double bond, a fragment with at least five carbon atoms. For example, 1-heptene forms considerably more aerosol than 3-heptene, and 2,4,4,-trimethyl-1-pentene (isooctene) forms more aerosol than its isomer, *trans*-4-octene. Cyclic olefins and diolefins form more aerosol than 1-alkenes that have the same number of carbon atoms. Heavier unsaturated cyclic compounds such as indene and terpenes lead to substantial amounts of aerosol when photooxidized.[132] Carbonyl compounds (ketones, C1–C7 aldehydes, dialdehydes) do not generate aerosol. Significant aerosol quantities are formed during the photooxidation of aromatic hydrocarbons.[130,131]

Natural hydrocarbons like the monoterpenes ($C_{10}H_{16}$) and isoprene (C_5H_8) are emitted by various types of trees and plants. In the U.S. biogenic hydrocarbon sources are estimated to produce 30–60 Mt of carbon per year (isoprene and monoterpenes combined) whereas anthropogenic hydrocarbon sources have been estimated to account for 27 Mt of carbon per year.[135] Laboratory investigations have indicated that biogenic hydrocarbons are very reactive under typical atmospheric conditions.[132,136,137] The aerosol forming potential of biogenic hydrocarbons has been investigated in a series of outdoor smog chamber studies.[132,138] Whereas isoprene photooxidation does not contribute to the production of secondary aerosol under ambient conditions, the terpenes form secondary aerosol in their reactions with O_3 and OH and have the potential to contribute significantly to aerosol in areas with high vegetation coverage. Monoterpenes have been estimated to contribute around 15% of the secondary organic aerosol in low vegetation urban areas like Los Angeles, while they are expected to dominate the secondary organic aerosol in areas with high vegetation coverage like Atlanta.[138]

Pandis et al.[139] estimated that the major secondary organic aerosol precursors in a typical Los Angeles smog episode are toluene, the xylene isomers, α- and β-pinene, higher alkanes with more than 15 carbon atoms, cresols, C10 to C15 alkenes,

nitrophenols, and trimethylbenzenes. Considering that during the photooxidation of each of these species several condensable products are formed, the ambient secondary organic aerosol in the urban atmosphere is expected to consist of dozens of chemical compounds coexisting with at least a like number of primary organic aerosol species. The enormous chemical complexity of the organic aerosol poses the most significant problem in our effort to understand its sources and the processes contributing to its formation.

Few measurements exist of the full spectrum of organic compounds in atmospheric aerosols and fewer yet of their size distribution. Pickle et al.[140] and Mylonas et al.[141] reported some measurements of secondary organic aerosol size distributions. Pandis et al.[142] found that accommodation coefficient differences could explain the observed bimodal distributions, but the further description of secondary organic aerosol dynamics awaits considerably more laboratory and ambient data.

Aqueous-Phase Chemical Reactions. Atmospheric liquid water existing either in the form of aerosols or water droplets can provide an additional reactive medium for the transformation of gaseous aerosol precursors to particulate matter. Several gaseous species dissolve in cloudwater and react giving products that are typically acidic and remain in the aerosol phase after the cloud dissipates. These species can attract additional gaseous species, for example ammonia and water, into the aerosol phase and therefore increase further the aerosol mass. Aerosol processing by nonprecipitating clouds represents a mechanism by which atmospheric particles can grow during their residence time in the atmosphere. The most important transformation is the oxidation of dissolved SO_2 (S(IV)) to sulfate.[143-151] The main reaction pathways for this transformation are the oxidation of S(IV) by H_2O_2, O_3, OH, and O_2 (catalyzed by Fe^{3+} and Mn^{2+}).[147] A review of the state of science in 1990 has been presented by US NAPAP.[152]

Atmospheric aerosols at high relative humidities (60−100%) may contain more than 100 $\mu g\ m^{-3}$ of liquid water.[104,153] Current knowledge of the sulfate production rates and pathways for solutions at such high concentrations (even at 99% relative humidity the aerosol solution has a total solute concentration of more than 1 M) is incomplete. Inhibition by the high ionic strength is expected for the ion−ion reactions.[154] Extrapolation of the reaction rates measured in dilute solutions to the high concentrations characteristic of aerosols have indicated that aerosol-phase sulfate production is of secondary importance in urban environments to gas—or droplet—phase processing.[153,155,156] However, as mentioned earlier, Sievering et al.[35] have shown that oxidation of SO_2 by ozone in alkaline sea-salt particles can be an important SO_2 sink and sulfate production pathway in the remote marine boundary layer. Similar rapid sulfate formation could take place in alkaline soil particles. Measurements of the sulfate production rates in ambient aerosol particles are needed to quantify the contribution of this sulfate production pathway.

Water droplets in clouds, fogs, or rain provide roughly 4 orders of magnitude more liquid water for sulfate production than do submicron aerosols and can be viewed literally as atmospheric microreactors. Processing of an air parcel by a cloud or fog can lead to significant sulfate production.[151,153,157-161] The detection of sulfate-producing reactions is often hindered by the variability of cloud liquid water content and the temporal instability and spatial variability in concentrations of reagents and product species.[162] Aqueous-phase oxidation of HSO_3^- by H_2O_2 is particularly fast, as evidenced by the mutual exclusivity of SO_2 and H_2O_2 observed in clouds.[163,164] The $SO_2(g)$ consumption rate resulting from its aqueous reaction with H_2O_2 in a typical cloud is around 1000% per hour.[147] Other reactions including oxidation of dissolved SO_2 by ozone and oxidation by O_2 catalyzed by Fe^{3+} and Mn^{2+} may also contribute, significantly in some cases, to sulfate production.[147,150,165]

Pandis et al.[153] demonstrated that the sulfate content of an air parcel passing for 1 h through a fog layer may more than double. Walcek et al.[166] calculated that during the passage of a midlatitude storm system over 65% of the sulfate in the troposphere over the northeastern United States was formed in cloud droplets via aqueous-phase chemical reactions. The same authors indicated that during a 3-day springtime period chemical reactions in clouds occupying 1−2% of the tropospheric volume were responsible for sulfate production comparable to the gas-phase reactions throughout the tropospheric volume under consideration. These conclusions are in quantitative agreement with more recent calculations.[167-169] Aqueous-phase oxidation in clouds is also the most important pathway for the conversion of SO_2 to sulfate on the global scale.[170,171] Clouds could under some conditions also be a significant source of aerosol nitrate during the night. Choularton et al.[172] and Colvill et al.[173] observed production of around 0.5 $\mu g\ m^{-3}$ of nitrate during the processing of an air parcel by a cloud. They speculated that the sources of this nitrate were gaseous N_2O_5 and NO_3.

A cyclical relationship between the occurrence of smog and fog in polluted areas has been termed the smog−fog−smog cycle.[174] A polluted atmosphere with high aerosol loading assists the formation of late night and early morning fogs that enhance aerosol sulfate the next day.[175-177] Processing of aerosol by clouds can result in similar cyclical relationships and contribution of the aerosol production in clouds to ground level particulate concentrations.[178]

6. Cloud Effects on Aerosol Size/Composition Distribution

Several measurements of the aerosol size distributions in urban areas have shown that two distinct modes can exist in the 0.1−1 μm diameter range,[179-182] referred to as the condensation mode (approximate aerodynamic diameter 0.2 μm) and the droplet mode (aerodynamic diameter around 0.7 μm). Hering and Friedlander[179] and John et al.[182] postulated that the larger mode could result from aqueous-phase chemistry. Meng and Seinfeld[156] demonstrated that growth of condensation mode particles by accretion of water vapor or by gas-phase or aerosol-phase sulfate production cannot explain the existence of the droplet mode. Instead, they showed that activation of condensation mode particles, subsequent chemical reactions in the resulting cloud/fog droplets, and finally droplet evaporation is a plausible mechanism for formation of the urban and regional aerosol droplet mode. The sulfate formed during fog/cloud processing of an air mass favors the aerosol particles that had access to most of the fog/cloud liquid water content, which are usually the particles with dry diameters around 1 μm.[183] This nonuniform distribution of the droplet-produced sulfate can clearly impact the radiative properties of the aerosol.[184,185]

The aerosol distribution is also modified during in-cloud processing by collision-coalescence of droplets and impaction scavenging of aerosols.[186] Aerosol scavenging by droplets is a relatively slow process, and collision coalescence among droplets of different sizes causes a redistribution of aerosol mass in such a manner that the main aerosol mass is associated with the main water mass.[187] Processing of remote aerosol by nonprecipitating clouds has been clearly demonstrated in a series of field studies.[34,187,188]

Despite the importance of the aerosol−droplet−aerosol cycle in accelerating the production of atmospheric acidity and shifting

the aerosol size distribution, quantitative understanding of this activation, reaction, and evaporation process remains limited. Traditionally, clouds have been the system of preference for the study of the aerosol–droplet interactions in the atmosphere. However, it has proven extremely difficult to isolate and examine a single process in a cloud. Cap cloud formation offers such an opportunity.[172] Fogs offer an analogous system to study.[159] While available models for aqueous-phase sulfate production have grown more and more complex, their predictive capabilities remain relatively untested as a result of the lack of appropriate data sets.

Chemical heterogeneities with respect to size in fog and cloud droplets affect significantly the overall sulfate production rate and the resulting sulfate size distribution.[153,189–200] Neglecting chemical concentration differences with size has been shown to result in significant underestimation of sulfate production rates in some cases.[192,197] Ice-related microphysical processes can have a significant impact on cloud chemistry.[201–203]

Enhanced aerosol concentrations in the vicinity of clouds have been observed.[204–207] Saxena and Hendler[204] suggested that these observations could be a result of the shattering of rapidly evaporating droplets. Enhanced actinic radiation fluxes near cloud tops have been proposed to lead to high OH concentrations and nucleation of H_2SO_4/H_2O particles.[207] High relative humidity areas around clouds often exhibit total particle number concentrations about twice those in air well removed from cloud boundaries.[206] These regions also provide areas for preferential nucleation.[102] Generation of new particles in the vicinity of clouds is not expected to contribute significantly to aerosol mass but may influence the shape of the aerosol number distribution, especially in remote regions.

7. Conclusions

The ability to model atmospheric processes involving trace gases and aerosols is crucial in predicting effects of changing anthropogenic emissions on urban and regional air pollution, global atmospheric chemistry, and global climate. A long-term goal is to incorporate fundamental atmospheric chemistry and physics into three-dimensional dynamical atmospheric models. This will include heterogeneous and condensed phase chemistry and full feedback between aerosol and cloud microphysics and atmospheric chemistry. Atmospheric aerosols have been implicated in human health effects on the urban scale, in visibility reduction on the urban and regional scale, and are now recognized as perhaps the single most important uncertainty in the anthropogenic contribution to global climate.

We have presented here a survey of the current state of understanding of the processes influencing the dynamics of atmospheric aerosols. Because of the wide variety of physical and chemical processes influencing aerosols, mathematical models of atmospheric aerosol dynamics are significantly more complex than those describing atmospheric trace gas behavior. Moreover, because of the difficulties in measuring the size/composition distribution of aerosols and because of their significant spatial and temporal variability in the troposphere, there exist at present relatively few data that can be used as a basis for evaluating the models that do exist.

Acknowledgment. The research upon which this article is based has been supported by National Science Foundation Grant ATM-9307603.

References and Notes

(1) Zhang, R.; Wooldridge, P. J.; Abbatt, J. P. D.; Molina, M. J. *J. Phys. Chem.* **1993**, *97*, 7351.
(2) Hamill, P.; Toon, O. B. *Phys. Today* **1991**, *44*, 34.
(3) Hofmann, D. J. *Science* **1990**, 996.
(4) Hansen, J. E.; Lacis, A.; Ruedy, R.; Sato, M. *Geophys. Res. Lett.* **1992**, *19*, 215.
(5) Dockery, D. W.; Pope, III, C. A.; Xu, X.; Spengler, J. D.; Ware, J. H.; Fay, M. E.; Ferris, Jr., B. G.; Speizer, F. E. *New England J. Med.* **1993**, *329*, 1753.
(6) Ball, R. J.; Robinson, G. D. *J. Appl. Meterol.* **1982**, *21*, 171.
(7) Eldering, A.; Larson, S. M.; Hall, J. R.; Hussey, K. J.; Cass, G. R. *Environ. Sci. Technol.* **1993**, *27*, 626.
(8) Liepert, B.; Fabian, P.; Grassl, H. *Beitr. Phys. Atmos.* **1994**, *67*, 15.
(9) *Acidic Deposition: State of Science and Technology*; NAPAP Office of the Director: Washington, DC, 1990.
(10) Charlson, R. J.; Schwartz, S. E.; Hales, J. M.; Cess. R. D.; Coakley, J. A.; Hansen, J. E.; Hofmann, D. J. *Science* **1992**, *255*, 422.
(11) Andreae, M. O. In *World Survey of Climatology*; Henderson-Sellers, A., Ed.; Elsevier: Amsterdam, 1995; Vol. XX.
(12) Penner, J. E.; Charlson, R. J.; Hales, J. M.; Laulainen, N. S.; Leifer, R.; Novakov, T.; Ogren, J.; Radke, L. F.; Schwartz, S. E.; Travis, L. *Bull. Am. Meteorol. Soc.* **1994**, *75*, 375.
(13) *Radiative Forcing of Climate Change*; Intergovernmental Panel on Climate Change, 1994.
(14) Heintzenberg, J. *Tellus* **1989**, *41B*, 149.
(15) Fitzgerald, J. W. *Atmos. Environ.* **1991**, *25A*, 533.
(16) Whitby, K. T.; Sverdrup, G. M. *Adv. Environ. Sci. Technol.* **1980**, *10*, 477.
(17) Jaenicke, R. In *Nucleation and Atmospheric Aerosols*; Fukuta, N., Wagner, P. E., Eds.; Deepak Publishing: Hampton, VA, 1992.
(18) Savoie, D. L.; Prospero, J. M. *Nature* **1989**, *339*, 685.
(19) Blanchard, D. C.; Woodcock, A. H. *Tellus* **1957**, *9*, 145.
(20) Monahan, E. C.; Fairall, C. W.; Davidson, K. L.; Jones-Boyle, P. *Q. J. R. Meteorol. Soc.* **1983**, *109*, 379.
(21) Blanchard, D. C.; Cipriano, R. J. *Nature* **1987**, *330*.
(22) O'Dowd, C. D.; Smith, M. H. *J. Geophys. Res.* **1993**, *98*, 1137.
(23) Charlson, R. J.; Lovelock, J. E.; Andreae, M. O.; Warren, S. G. *Nature* **1987**, *326*, 655.
(24) Yin, F. D.; Grosjean, D.; Seinfeld, J. H. *J. Atmos. Chem.* **1990**, *11*, 309.
(25) Yin, F. D.; Grosjean, D.; Flagan, R. C.; Seinfeld, J. H. *J. Atmos. Chem.* **1990**, *11*, 365.
(26) Berresheim, H.; Eisele, F. L.; Tanner, D. J.; McInnes, L. M.; Ramseybell, D. C. *J. Geophys. Res.* **1993**, *98*, 12701.
(27) Bandy, A. R.; Scott, D. L.; Blomquist, B. W.; Chen, S. M.; Thornton, D. C. *Geophys. Res. Lett.* **1992**, *19*, 1125.
(28) Kreidenweis, S. M.; Penner, J. E.; Yin, F.; Seinfeld, J. H. *Atmos. Environ.* **1991**, *25*, 2501.
(29) Kreidenweis, S. M.; Yin, F. D.; Wang, S. C.; Grosjean, D.; Flagan, R. C. *Atmos. Environ.* **1991**, *25*, 2491.
(30) Pandis, S. N.; Russell, L. M.; Seinfeld, J. H. *J. Geophys. Res.* **1994**, *99*, 16945.
(31) Russell, L. M.; Pandis, S. N.; Seinfeld, J. H. *J. Geophys. Res.* **1994**, *99*, 20989.
(32) Perry, K. D.; Hobbs, P. V. *J. Geophys. Res.* **1994**, *99*, 22803.
(33) Hoppel, W. A.; Fitzgerald, J. W.; Larson, R. E. *J. Geophys. Res.* **1985**, *90*, 2365.
(34) Hoppel, W. A.; Frick, G. M.; Larson, R. E. *Geophys. Res. Lett.* **1986**, *13*, 125.
(35) Sievering, H.; Boatman, J.; Gorman, E.; Kim, Y.; Anderson, L.; Ennis, G.; Luria, M.; Pandis, S. N. *Nature* **1992**, *360*, 571.
(36) Deepak, A.; Gali, G. *The International Global Aerosol Program (IGAP) Plan*; Deepak Publishing: Hampton, VA, 1991.
(37) Bashurova, V. S.; Dreiling, V.; Hodger, T. V.; Jaenicke, R.; Koutsenogii, K. P.; Koutsenogii, P. K.; Kraemer, M.; Makarov, V. I.; Obolkin, V. A.; Potjomkin, V. L.; Pusep, A. Y. *J. Aerosol Sci.* **1992**, *23*, 191.
(38) Koutsenogii, P. K.; Bufetov, N. S.; Drosdova, V. I. *Atmos. Environ.* **1993**, *27*, 1629.
(39) Koutsenogii, P. K.; Jaenicke, R. *J. Aerosol Sci.* **1994**, *25*, 377.
(40) Prospero, J. In *The Long-Range Atmospheric Transport of Natural and Contaminant Substances*; NATO ASI Series; Knap, A. H., Ed.; Kluwer Acadaemic Publishes: New York, 1990; pp 59–82.
(41) Glavas, S. *Atmos. Environ.* **1988**, *22*, 1505.
(42) Wefers, M.; Jaenicke, R. In *Aerosols*; Masuda, S., Takahashi, K., Eds.; Pergamon Press: New York, 1990; pp 1086–1089.
(43) Browell, E. V.; Butler, C. F.; Kooi, S. A.; Fenn, M. A.; Harriss, R. C.; Gregory, G. L. *J. Geophys. Res.* **1992**, *97*, 16433.
(44) Barrie, L. A. *Atmos. Environ.* **1986**, *29*, 643.
(45) Talbot, R. W.; Vijgen, A. S.; Harris, R. C. *J. Geophys. Res.* **1992**, *97*, 16531.
(46) Kleinman, L. I.; Daum, P. H. *J. Geophys. Res.* **1991**, *96*, 991.
(47) Leaitch, W. R.; Isaac, G. A. *Atmos. Environ.* **1991**, *25A*, 601.
(48) Clarke, A. D. *J. Atmos. Chem.* **1993**, *14*, 479.
(49) Hofmann, D. J. *J. Geophys. Res.* **1993**, *98*, 12753.

(50) Andreae, M. O.; Anderson, B. E.; Blake, D. R.; Bradshaw, J. D.; Collins, J. E.; Gregory, G. L.; Sasche, G. W.; Shipham, M. C. *J. Geophys. Res.* **1994**, *99*, 12793.
(51) Anderson, B. E.; Gregory, G. L.; Barrick, J. D. W.; Collins, J. E.; Sachse, G. W.; Bagwell, D.; Shipham, M. C.; Bradshaw, J. D.; Sandholm, S. T. *J. Geophys. Res.* **1993**, *98*, 23477.
(52) Fuchs, N. A. *The Mechanics of Aerosols*; Dover Publications: New York, 1989.
(53) Stull, R. B. *An Introduction to Boundary Layer Meteorology*; Kluwer: Dordrecht, 1988.
(54) Seinfeld, J. H. *Atmospheric Chemistry and Physics of Air Pollution*; Wiley: New York, 1986.
(55) Grad, H. In *Encyclopedia of Physics*; Flugge, S., Ed.; Springer: Berlin, 1958; Vol. 12, pp 205−294.
(56) Fuchs, N. A.; Sutugin, A. G. In *Topics in Current Aerosol Research*; Hidy, G. M., Brock, J. R., Eds.; Pergamon: New York, 1971; pp 1−60.
(57) Sitarski, M.; Nowakowski, B. *J. Colloid Interface Sci.* **1979**, *72*, 112.
(58) Tompson, R. V.; Loyalka, S. K. *J. Aerosol Sci.* **1988**, *3*, 287.
(59) Monchick, L.; Blackmore, R. *J. Aerosol Sci.* **1988**, *19*, 273.
(60) Loyalka, S. K.; Hamoodi, S. A.; Tompson, R. V. *Phys. Fluids A* **1989**, *1*, 358.
(61) Wexler, A. S.; Seinfeld, J. H. *Atmos. Environ.* **1990**, *24A*, 1231.
(62) Young, J. B. *Int. J. Heat Mass Transfer* **1993**, *36*, 2941.
(63) Wagner, P. E. In *Aerosol Microphysics II. Chemical Physics of Microparticles*; Marlow, W. H., Ed.; Springer-Verlag: Berlin, 1982.
(64) Davis, E. J. *Aerosol Sci. Technol.* **1983**, *2*, 121.
(65) Loyalka, S. K.; Griffin, J. L. *Nucl. Sci. Eng.* **1993**, *114*, 135.
(66) Jayne, J. T.; Davidovits, P.; Worsnop, D. R.; Zahniser, M. S.; Kolb, C. E. *J. Phys. Chem.* **1990**, *94*, 6041.
(67) Jayne, J. T.; Duan, S. X.; Davidovits, P.; Worsnop, D. R.; Zahniser, M. S.; Kolb, C. E. *J. Phys. Chem.* **1992**, *96*, 5452.
(68) De Bruyn, W. J.; Shorter, J. A.; Davidovits, P.; Worsnop, D. R.; Zahniser, M. S.; Kolb, C. E. *J. Geophys. Res.* **1994**, *99*, 16927.
(69) Mozurkewich, M. *Aerosol Sci. Technol.* **1986**, *5*, 223.
(70) Schwartz, S. E. In *Chemistry of Multiphase Atmospheric Systems*; Jaeschke, W., Ed.; Springer-Verlag: Berlin, 1986; pp 415−471.
(71) Hightower, R. L.; Richardson, C. B. *Atmos. Environ.* **1988**, *22*, 2587.
(72) Gill, P. S.; Graedel, T. E.; Weschler, C. J. *Rev. Geophys. Space Phys.* **1983**, *21*, 903.
(73) Tseng, R.-S.; Viechnicki, J. T.; Skop, R. A.; Brown, J. W. *J. Geophys. Res.* **1992**, *97*, 5201.
(74) Barger, W. R.; Garrett, W. D. *J. Geophys. Res.* **1970**, *75*, 4561.
(75) Barger, W. R.; Garrett, W. D. *J. Geophys. Res.* **1976**, *81*, 3151.
(76) Garrett, W. D. *J. Atmos. Sci.* **1971**, *28*, 816.
(77) Blanchard, D. C. *Science* **1964**, *146*, 396.
(78) Daumer, B.; Niessner, R.; Klockow, D. *J. Aerosol Sci.* **1992**, *23*, 325.
(79) Rubel, G. O.; Gentry, J. W. *J. Aerosol Sci.* **1985**, *16*, 571.
(80) Kim, Y. P.; Seinfeld, J. H.; Saxena, P. *Aerosol Sci. Technol.* **1993**, *19*, 157.
(81) Kim, Y. P.; Seinfeld, J. H.; Saxena, P. *Aerosol Sci. Technol.* **1993**, *19*, 182.
(82) Wexler, A. S.; Seinfeld, J. H. *Atmos. Environ.* **1991**, *25A*, 2731.
(83) Wexler, A. S. In *CRC Handbook of Chemistry and Physics*; Lide, D. R., Ed.; CRC Press: Boca Raton, FL, 1992.
(84) Cohen, M. D.; Flagan, R. C.; Seinfeld, J. H. *J. Phys. Chem.* **1987**, *91*, 4563.
(85) Kim, Y. P.; Pun, B. K.-L.; Chan, C. K.; Flagan, R. C.; Seinfeld, J. H. *Aerosol Sci. Technol.* **1994**, *20*, 275.
(86) Richardson, C. B.; Spann, J. F. *J. Aerosol Sci.* **1984**, *15*, 563.
(87) Cohen, M. D.; Flagan, R. C.; Seinfeld, J. H. *J. Phys. Chem.* **1987**, *91*, 4575.
(88) Chan, C. K.; Flagan, R. C.; Seinfeld, J. H. *Atmos. Environ.* **1992**, *26A*, 1661.
(89) Spann, J. F.; Richardson, C. B. *Atmos. Environ.* **1985**, *19*, 819.
(90) Pitzer, K. S. *Pure Appl. Chem.* **1986**, *58*, 1599.
(91) Clegg, S. L.; Pitzer, K. S. *J. Phys. Chem.* **1992**, *96*, 3513.
(92) Clegg, S. L.; Pitzer, K. S. *J. Phys. Chem.* **1992**, *96*, 9470.
(93) Kusik, C. L.; Meissner, H. P. *AIChE Symp.* **1978**, *173*, 14.
(94) Bromley, L. A. *AIChE J.* **1973**, *19*, 313.
(95) Andrews, E.; Larson, S. M. *Environ. Sci. Technol.* **1993**, *27*, 857.
(96) Hansson, H. C.; Wiedensohler, A.; Rood, M. J.; Covert, D. S. *J. Aerosol Sci.* **1990**, *21*, S241.
(97) Wexler, A. S.; Seinfeld, J. H. *Atmos. Environ.* **1992**, *26A*, 579.
(98) Wyslouzil, B. E.; Seinfeld, J. H.; Flagan, R. C.; Okuyama, K. *J. Chem. Phys.* **1991**, *94*, 6842.
(99) Jaecker-Voirol, A.; Mirabel, P. *Atmos. Environ.* **1989**, *23*, 2053.
(100) Wexler, A. S.; Lurmann, F. W.; Seinfeld, J. H. *Atmos. Environ.* **1994**, *28*, 531.
(101) Kerminen, V.-M.; Wexler, A. S. *Atmos. Environ.* **1994**, *28*, 2399.
(102) Kerminen, V.-M.; Wexler, A. S. *J. Geophys. Res.* **1994**, *99*, 25607.
(103) Kerminen, V.-M.; Wexler, A. S. *Atmos. Environ.*, in press.
(104) Pilinis, C.; Seinfeld, J. H. *Atmos. Environ.* **1987**, *21*, 2453.
(105) Flagan, R. C. In *Measurement Challenges in Atmospheric Chemistry*; Newman, L., Ed.; American Chemical Society: Washington, DC, 1993.
(106) McKeown, P. J.; Johnston, M. V.; Murphy, D. M. *Anal. Chem.* **1991**, *63*, 2069.
(107) Thompson, D. S.; Murphy, D. M. *Appl. Opt.* **1993**, *32*, 6818.
(108) Prather, K. A.; Nordmeyer, T.; Salt, K. *Anal. Chem.* **1994**, *66*, 1403.
(109) Mansoori, B. A.; Johnston, M. V.; Wexler, A. S. *Anal. Chem.* **1994**, *66*, 3681.
(110) Carson, P. G.; Neubauer, K. R.; Johnston, M. V.; Wexler, A. S. *J. Aerosol Sci.*, in press.
(111) Pilinis, C. *Atmos. Environ.* **1990**, *24A*, 1928.
(112) Whitby, E. R.; McMurry, P. H.; Shankar, U.; Binkowski, F. S. *Model Aerosol Dynamics Modeling*; Atmospheric Research and Exposure Assessment Laboratory, Office of Research and Development, U.S.E.P.A.: Research Triangle Park, NC, 1991.
(113) Kim, Y. P.; Seinfeld, J. H. *J. Colloid Interface Sci.* **1992**, *149*, 425.
(114) McRae, G. J.; Goodin, W. R.; Seinfeld, J. H. *J. Comput. Phys.* **1982**, *45*, 1.
(115) Dabdub, D.; Seinfeld, J. H. *Atmos. Environ.* **1994**, *28*, 3369.
(116) Slinn, W. G. N. In *Atmospheric Sciences and Power Production−1979*; Division of Biomedical Environmental Research, USDOE, 1983.
(117) Keene, W. C.; Pszenny, A. A. P.; Jacob, D. J.; Duce, R. A.; Galloway, J. N.; Schultz-Tokos, J. J.; Sievering, H.; Boatman, J. F. *Global Biogeochem. Cycles* **1990**, *4*, 407.
(118) De More, W. B.; Sander, S. P.; Golden, D. M.; Molina, M. J.; Hampson, R. F.; Kurylo, M. J.; Howard, C. J.; Ravishankara, A. R. Jet Propulsion Laboratory Publications, 90-1; Pasadena, CA, 1990.
(119) Anderson, L. G.; Gates, P. M.; Nold, C. R. In *Biogenic Sulfur in the Environment*; Saltzman, E. S., Cooper, W. J., Eds.; ACS Symp. Ser. No. 393; American Chemical Society: Washington, DC, 1989.
(120) Kolb, C. E.; Jayne, J. T.; Worsnop, D. R.; Molina, M. J.; Meads, R. F.; Viggians, A. A. *J. Am. Chem. Soc.* **1994**, *116*, 10314.
(121) Lovelock, J. E. *Gaia: A New Look at Life on Earth*; Oxford University Press: Oxford, 1979.
(122) Ayers, G. P.; Gras, J. L. *Nature* **1991**, *353*, 834.
(123) Clarke, A. D.; Alquist, N. C.; Covert, D. S. *J. Geophys. Res.* **1987**, *92*, 4179.
(124) Lin, X.; Chameides, W. L. *Geophys. Res. Lett.* **1993**, *20*, 579.
(125) Kreidenweis, S. M.; Seinfeld, J. H. *Atmos. Environ.* **1988**, *22*, 283.
(126) Lawrence, M. G. *J. Geophys. Res.* **1993**, *98*, 20663.
(127) Atkinson, R. *J. Phys. Chem. Ref. Data, Monogr.* **1994**, *2*, 1.
(128) Atkinson, R. *J. Phys. Chem. Ref. Data* **1991**, *20*, 459.
(129) Grosjean, D.; Seinfeld, J. H. *Atmos. Environ.* **1989**, *23*, 1733.
(130) Wang, S. C.; Paulson, S. E.; Grosjean, D.; Flagan, R. C.; Seinfeld, J. H. *Atmos. Environ.* **1992**, *26A*, 403.
(131) Wang, S. C.; Flagan, R. C.; Seinfeld, J. H. *Atmos. Environ.* **1992**, *26A*, 421.
(132) Zhang, S. H.; Shaw, M.; Seinfeld, J. H.; Flagan, R. C. *J. Geophys. Res.* **1992**, *97*, 20717.
(133) Grosjean, D.; Friedlander, S. K. *J. Air Pollut. Control Assoc.* **1975**, *25*, 1038.
(134) O'Brien, R. J.; Crabtree, J. H.; Holmes, J. R.; Hoggan, M. C.; Bockian, A. H. *Environ. Sci. Technol.* **1975**, *9*, 577.
(135) Lamb, B.; Guenther, A.; Gay, D.; Westberg, H. *Atmos. Environ.* **1987**, *21*, 1695.
(136) Paulson, S. E.; Flagan, R. C.; Seinfeld, J. H. *Int. J. Chem. Kinet.* **1992**, *24*, 79.
(137) Paulson, S. E.; Flagan, R. C.; Seinfeld, J. H. *Int. J. Chem. Kinet.* **1992**, *24*, 103.
(138) Pandis, S. N.; Paulson, S. E.; Seinfeld, J. H.; Flagan, R. C. *Atmos. Environ.* **1991**, *25A*, 997.
(139) Pandis, S. N.; Harley, R. A.; Cass, G. R.; Seinfeld, J. H. *Atmos. Environ.* **1992**, *26A*, 2269.
(140) Pickle, T.; Allen, D. T.; Pratsinis, S. E. *Atmos. Environ.* **1990**, *24*, 2221.
(141) Mylonas, D. T.; Allen, D. T.; Ehrman, S. H.; Pratsinis, S. E. *Atmos. Environ.* **1991**, *25A*, 2855.
(142) Pandis, S. N.; Wexler, A. S.; Seinfeld, J. H. *Atmos. Environ.* **1993**, *27A*, 2403.
(143) Chameides, W. L.; Davis, D. D. *J. Geophys. Res.* **1982**, *87*, 4863.
(144) Chameides, W. L. *J. Geophys. Res.* **1984**, *89*, 4739.
(145) Seigneur, C.; Saxena, P. *Atmos. Environ.* **1984**, *18*, 2109.
(146) Jacob, D. J. *J. Geophys. Res.* **1986**, *91*, 9807.
(147) Pandis, S. N.; Seinfeld, J. H. *J. Geophys. Res.* **1989**, *94*, 1105.
(148) Forkel, R.; Seidl, W.; Dlugi, R.; Deigele, E. *J. Geophys. Res.* **1990**, *95*, 18501.
(149) Bott, A. *Bound Layer Met.* **1991**, *56*, 1.
(150) Barth, M. C. *J. Appl. Met.* **1994**, *33*, 855−868.
(151) Devalk, J. P. *Atmos. Environ.* **1994**, *28*, 1665.

(152) *Acidic Deposition: State of Science and Technology*; Irving, P. M., Ed.; United States National Acid Precipitation Assessment Program: Washington, DC, 1991; Vol. I.
(153) Pandis, S. N.; Seinfeld, J. H.; Pilinis, C. *Atmos. Environ.* **1992**, *26A*, 2509.
(154) Martin, L. R.; Hill, M. W. *Atmos. Environ.* **1987**, *21*, 1487.
(155) Saxena, P.; Seigneur, C. *Atmos. Environ.* **1987**, *21*, 807.
(156) Meng, Z.; Seinfeld, J. H. *Aerosol Sci. Technol.* **1994**, *20*, 253.
(157) Hegg, D. A.; Hobbs, P. V. *Geophys. Res. Lett.* **1987**, *14*, 719.
(158) Hegg, D. A.; Hobbs, P. V. *J. Atmos. Chem.* **1988**, *7*, 325.
(159) Pandis, S. N.; Seinfeld, J. H. *J. Geophys. Res.* **1989**, *94*, 12911.
(160) Husain, L.; Dutkiewisz, V. A.; Hussain, M. M.; Khwaja, H. A.; Burkhard, E. G.; Mehmood, G.; Parekh, P. P.; Canelli, E. *J. Geophys. Res.* **1991**, *96*, 8789.
(161) Liu, P. S. K.; Leaitch, W. R.; McDonald, A. M.; Isaac, G. A.; Strapp, J. W.; Wiebe, H. A. *Tellus* **1994**, *45*, 368.
(162) Kelly, T. J.; Schwartz, S. E.; Daum, P. H. *Atmos. Environ.* **1989**, *23*, 569.
(163) Daum, P. H.; Schwartz, S. E.; Newman, L. *J. Geophys. Res.* **1984**, *89*, 1447.
(164) Daum, P. H.; Kelly, T. J.; Strapp, J. W.; Leaitch, W. R.; Joe, P.; Schemenauer, R. S.; Isaac, G. A.; Anlauf, K. G.; Wiebe, H. A. *J. Geophys. Res.* **1987**, *92*, 8426.
(165) Barth, M. C.; Hegg, D. A.; Hobbs, P. V. *J. Geophys. Res.* **1992**, *97*, 5825.
(166) Walcek, C. J.; Stockwell, W. R.; Chang, J. S. *Atmos. Res.* **1990**, *25*, 53−69.
(167) McHenry, J. N.; Dennis, R. L. *J. Appl. Meteorol.* **1994**, *33*, 890.
(168) Dennis, R. L.; McHenry, J. N.; Barchet, W. R.; Binkowski, F. S.; Byun, D. W. *Atmos. Environ.* **1993**, *27*, 975.
(169) Karamachandani, P.; Venkatram, A. *Atmos. Environ.* **1992**, *26*, 1041.
(170) Hegg, D. A. *J. Geophys. Res.* **1985**, *90*, 3773.
(171) Langner, J.; Rodhe, H. *J. Atmos. Sci.* **1991**, *13*, 225.
(172) Choularton, T. W.; Wicks, A. J.; Dower, R. M.; Gallacher, M. W.; Penkett, S. A.; Bandy, B. J.; Dollard, G. J.; Jones, B. M. R.; Davies, T. D. *Environ. Pollut.* **1992**, *75*, 69.
(173) Colvill, R. N.; Choularton, T. W.; Gallagher, M. W.; Wicks, A. J.; Dover, R. M.; Tyler, B. J.; Storetownwest, K. J.; Fowler, D.; Cape, J. N. *Atmos. Environ.* **1994**, *28*, 397.
(174) Munger, J. W.; Jacob, D. J.; Waldman, J. M.; Hoffmann, M. R. *J. Geophys. Res.* **1983**, *88*, 5109.
(175) Cass, G. R. *Atmos. Environ.* **1979**, *13*, 1069−1084.
(176) Cass, G. R.; Shair, F. H. *J. Geophys. Res.* **1984**, *89*, 1429.
(177) Pandis, S. N.; Seinfeld, J. H.; Pilinis, C. *J. Geophys. Res.* **1990**, *95*, 18489−18500.
(178) Altshuller, A. P. *Atmos. Environ.* **1987**, *21*, 1097.
(179) Hering, S. V.; Friedlander, S. K. *Atmos. Environ.* **1982**, *16*, 2647.
(180) McMurry, P. H.; Wilson, J. C. *J. Geophys. Res.* **1983**, *88*, 5101.
(181) Wall, S. M.; John, W.; Ondo, J. L. *Atmos. Environ.* **1988**, *22*, 1649.
(182) John, W.; Wall, S. M.; Ondo, J. L.; Winklmayr, W. *Atmos. Environ.* **1990**, *24A*, 2349.
(183) Pandis, S. N.; Seinfeld, J. H.; Pilinis, C. *Atmos. Environ.* **1990**, *24A*, 1957.
(184) Hegg, D. A.; Yuen, P. F.; Larson, T. V. *J. Geophys. Res.* **1992**, *97*, 12927.
(185) Bower, K. N.; Choularton, T. W. *Q. J. R. Meteorol. Soc.* **1993**, *119*, 655.
(186) Pruppacher, H. R.; Klett, J. D. *Microphysics of Clouds and Precipitation*; Reidel: Dordrecht, 1980.
(187) Flossmann, A. I.; Hall, W. D.; Pruppacher, H. R. *J. Atmos. Sci.* **1985**, 583.
(188) Frick, G. M.; Hoppel, W. A. *Bull. Am. Meteorol. Soc.* **1993**, *74*, 2195.
(189) Seidl, W. *Tellus* **1989**, *41B*, 32.
(190) Twohy, C. H.; Austin, P. H.; Charlson, R. J. *Tellus* **1989**, *41B*, 51.
(191) Ayers, G. P.; Larson, T. V. *J. Atmos. Chem.* **1990**, *11*, 143.
(192) Hegg, D. A.; Larson, T. V. *Tellus* **1990**, *42B*, 272.
(193) Bower, K. N.; Hill, T. A.; Coe, H.; Choularton, T. W. *Atmos. Environ.* **1991**, *25*, 2401.
(194) Ogren, J. A.; Charlson, R. J. *Tellus* **1992**, *44*, 208.
(195) Roelofs, G. J. *J. Atmos. Chem.* **1992**, *14*, 109.
(196) Roelofs, G. J. *Atmos. Environ.* **1992**, *26A*, 2309.
(197) Roelofs, G. J. *Atmos. Environ.* **1993**, *27A*, 2255.
(198) Carter, E. J.; Borys, R. D. *J. Atmos. Chem.* **1993**, *17*, 277.
(199) Bott, A.; Carmichael, G. R. *Atmos. Environ.* **1993**, *27*, 503−522.
(200) Collett, J. L.; Oberholzer, B.; Staehelin, J. *Atmos. Environ.* **1993**, *27*, 33−42.
(201) Taylor, G. R. *J. Atmos. Sci.* **1989**, *46*, 1991.
(202) Wang, C.; Chang, J. S. *J. Geophys. Res.* **1993**, *98*, 16799.
(203) Collett, J. L.; Oberholzer, B.; Mosimann, L.; Staehelin, J.; Waldrogel, A. *Water, Air, Soil Pollut.* **1993**, *68*, 43.
(204) Saxena, V. K.; Hendler, A. H. In *Precipitation Scavenging, Dry Deposition and Resuspension*; Pruppacher, H. R., Semonin, R. G., Slinn, W. G. N., Eds.; Elsevier: New York, 1983; pp 91−102.
(205) Hegg, D. A.; Radke, L. F.; Hobbs, P. V. *J. Geophys. Res.* **1990**, *95*, 13917.
(206) Radke, L. F.; Hobbs, P. V. *J. Atmos. Sci.* **1991**, *48*, 1190.
(207) Hegg, D. A.; Radke, L. F.; Hobbs, P. V. *J. Geophys. Res.* **1991**, *96*, 18727.

JP950410N